Design, Synthesis, and Evaluation of Acrylamide Derivatives as Direct NLRP3 Inflammasome Inhibitors

Cocco, Mattia; Miglio, Gianluca; Giorgis, Marta; Garella, Davide; Marini, Elisabetta; Costale, Annalisa; Regazzoni, Luca; Vistoli, Giulio; Orioli, Marica; Massulaha-Ahmed, Raïhane; Détraz-Durieux, Isabelle; Groslambert, Marine; Py, Bénédicte F.; Bertinaria, Massimo. Design, Synthesis, and Evaluation of Acrylamide Derivatives as Direct NLRP3 Inflammasome Inhibitors. CHEMMEDCHEM. 11 (16) pp: 1790-1803.
DOI: 10.1002/cmdc.201600055

Design, Synthesis, and Evaluation of Acrylamide Derivatives as Direct NLRP3 Inflammasome Inhibitors

Mattia Cocco,[a] Gianluca Miglio,[a] Marta Giorgis,[a] Davide Garella,[a] Elisabetta Marini,[a] Annalisa Costale,[a] Luca Regazzoni,[b] Giulio Vistoli,[b] Marica Orioli,[b] Raïhane Massulaha-Ahmed,[c] Isabelle Détraz-Durieux,[c] Marine Groslambert,[c] Bénédicte F. Py,[c] and Massimo Bertinaria*[a]

[a] MSc M. Cocco (ORCID 0000-0003-4358-8599), Dr G. Miglio (ORCID 0000-0002-6602-2099), Dr M. Giorgis (ORCID 0000-0002-3282-1220), Dr D. Garella (ORCID 0000-0002-9455-8317), Dr E. Marini (ORCID 0000-0002-3638-5219), MSc A. Costale (ORCID 0000-0002-8590-5196), Prof M. Bertinaria (ORCID 0000-0002-2533-5830)
Dipartimento di Scienza e Tecnologia del Farmaco
Università degli Studi di Torino
Via P. Giuria 9, 10125 Torino (Italy)
E-mail: massimo.bertinaria@unito.it

[b] Dr L. Regazzoni (ORCID 0000-0001-7199-7141), Prof G. Vistoli (ORCID 0000-0002-3939-5172), Prof M. Orioli (ORCID 0000-0003-1558-9551)
Dipartimento di Scienze Farmaceutiche
Università degli Studi di Milano
Via Mangiagalli 25, 20133 Milano (Italy)

[c] MSc R. Massulaha-Ahmed (ORCID 0000-0003-0482-8780), BSc I. Détraz-Durieux (ORCID 0000-0003-0960-3548), MSc M. Groslambert (ORCID 0000-0003-3258-0268), Dr B. F. Py (ORCID 0000-0001-6716-7807)
CIRI, International Center for Infectiology Research, Inserm U1111, CNRS UMR 5308
Ecole Normale Supérieure de Lyon, Université Lyon 1
21 avenue Tony Garnier, 69007 Lyon, France

Supporting information for this article is given via a link at the end of the document.

Abstract: NLRP3 inflammasome plays a key role in the intracellular activation of caspase-1, processing of pro-inflammatory interleukin-1β (IL-1β), and pyroptotic cell death cascade. NLRP3 overactivation is implicated in the pathogenesis of autoinflammatory diseases, known as cryopyrin-associated periodic syndromes (CAPS), and in the progression of several diseases, such as atherosclerosis, type-2 diabetes, gout, and Alzheimer's disease. In this study, the synthesis of acrylamide derivatives and their pharmaco-toxicological evaluation as potential inhibitors of NLRP3-dependent events are described. Five hits were identified and evaluated for their efficiency in inhibiting IL-1β release from different macrophage subtypes, including CAPS mutant macrophages. Most attractive hits were tested for their ability to inhibit NLRP3 ATPase activity on human recombinant NLRP3. This screening allowed the identification of **14**, 2-(2-chlorobenzyl)-*N*-(4-sulfamoylphenethyl)acrylamide, able to concentration-dependently inhibit NLRP3 ATPase with an IC_{50} of 74 μM. The putative binding pose of **14** in the ATPase domain of NLRP3 is also proposed.

Introduction

Inflammation is a key physiological response to harmful stimuli, including exogenous pathogens and endogenous danger signals. Cells of the innate immune system recognize pathogen-associated molecular patterns (PAMPs) and danger-associated molecular patterns (DAMPs) through germline-encoded pattern recognition receptors (PRRs), such as Toll-like receptors (TLRs) and NOD-like receptors (Nucleotide-binding domain and leucine-rich repeat gene; NLRs).[1,2] A vast array of PAMPs and DAMPs has been recognized so far, including microbial products (e.g., lipopolysaccharide; LPS), molecules released after cell lysis (e.g., ATP),[3,4] hypotonic stress,[5,6] and particles produced as a consequence of an altered metabolism, such as cholesterol crystals,[7] sodium monourate crystals,[8] β-amyloid aggregates.[9] Despite the well-established protective role, uncontrolled and/or protracted inflammation is thought to exert detrimental effects, by both exacerbating underlying pathological processes and promoting the onset of new disorders.
In the last decades several studies have highlighted the pivotal role of inflammasomes, which are large intracellular protein complexes, in the molecular control of inflammatory processes.[10-12] In particular, the NLR family pyrin domain-containing 3 (NLRP3) inflammasome is the best characterized and the most widely implicated PRR in the caspase-1-dependent pro-inflammatory events, including both interleukin (IL)-1β maturation and cell death by pyroptosis. The pathological role of NLRP3 inflammasome activation has been better established in a subset of genetic disorders known as cryopyrin-associated periodic syndromes (CAPS), aka cryopyrinopathies. CAPS are characterized by recurrent episodes of severe systemic inflammation and have been related to the presence of gain-of-function mutations in the *NLRP3* gene.[13-15] NLRP3 and oligomeric ASC

particles have also been detected in the serum of patients with active CAPS, where they mediate the amplification of the inflammatory response.[16] Moreover, compelling data have implicated inflammasome activation in the progression of several noncommunicable diseases, such as atherosclerosis,[7] type-2 diabetes mellitus,[17] gout,[8] and Alzheimer's disease.[18]
These evidences have risen the interest toward the discovery of agents able to prevent inflammasome activation, which is regarded as a promising therapeutic strategy to reduce chronic inflammation and associated damage in different pathological settings. To date, different approaches have been pursued,[19] among which reversible or irreversible modification of reactive cysteine (Cys) residues of relevant proteins seems to be the prevalent one. Structure-based drug design would help in the development of safer covalent drugs targeting suitably positioned Cys residues. However, structural knowledge of NLRP3 is still to be fully understood: apart from the disulfide bridge between Cys8 and Cys108 in NLRP3-PYD domain, little is known on the other 43 Cys residues of NLRP3 (Uniprot ID: Q96P20-1).
Crystal structure of NLRP3 ATPase active site is not yet available, nonetheless, this pocket in the NACHT domain could be an interesting target to develop NLRP3 inhibitors,[20] in fact ATP hydrolysis is required to have active NLRP3 in the cytosol.[21]
In a previous study, our group developed a series of electrophilic warheads preventing the NLRP3-dependent and ATP-triggered cell death of differentiated and primed THP-1 cells, which is a cellular model of macrophage pyroptosis.[22] This proof of concept study demonstrated that molecules endowed with the ability to behave as Michael acceptors could efficiently prevent pyroptotic cell death by inhibiting NLRP3 signaling. A complex mechanism involving a multi-target action due to the reactivity of the electrophile could explain this effect.
The most promising warheads identified (Figure 1, compounds **1**-**3**) also proved able to directly inhibit the NLRP3 ATPase activity of isolated enzyme.

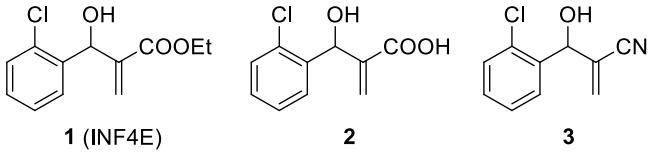

1 (INF4E) **2** **3**

Figure 1. Electrophilic warheads preventing NLRP3-dependent pyroptosis and inhibiting NLRP3 ATPase activity.

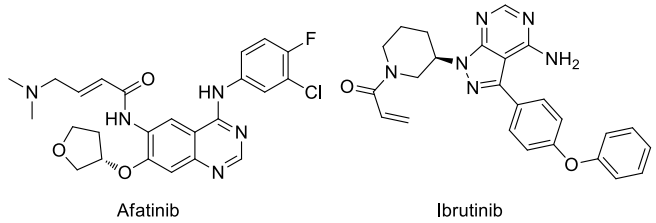

Afatinib Ibrutinib

Figure 2. Structures of approved acrylamide-based kinase inhibitors.

Molecules depicted in Figure 3 were designed by modulation of general structure **I**.
In this series of compounds we maintained the *o*-chloro-substituted benzene ring, which was previously identified as the optimal aromatic portion in acrylate-based inhibitors,[22] in the western part of the molecules. To investigate the role of the hydroxyl group in the reactivity and/or the cytotoxicity of this class of electrophilic compounds, a small set of *N*-substituted compounds bearing a hydroxyl group in benzylic position (compounds **4**−**7**) was synthesized and compared with a series of close analogues deprived of the hydroxyl group (compounds **8**, **9**, **11**). The OH group removal was then coupled to different *N*-substitution patterns (compounds **10**, **12**−**16**) to explore the possibility of increasing activity through direct NLRP3 inhibition.

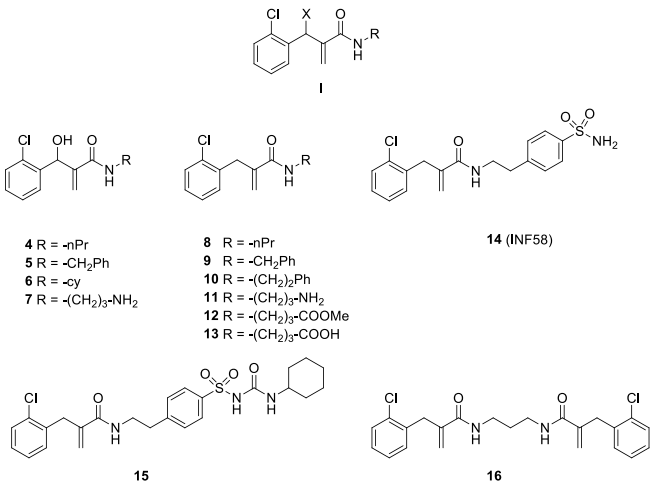

Figure 3. General structure **I** and chemical structures of designed compounds.

In particular, compounds **14** (INF58) and **15** were designed using a ligand merging strategy. Both **14** and **15** share the Michael acceptor moiety present in compound **1** (INF4E) and a sulfonamide or a sulfonylurea portion typical of compound 16673-34-0[24] and glyburide,[25] two known NLRP3-network inhibitors (Figure 4). Finally, the molecular pharmacophore dimerization strategy was considered in the design of compound **16** (Figure 3).

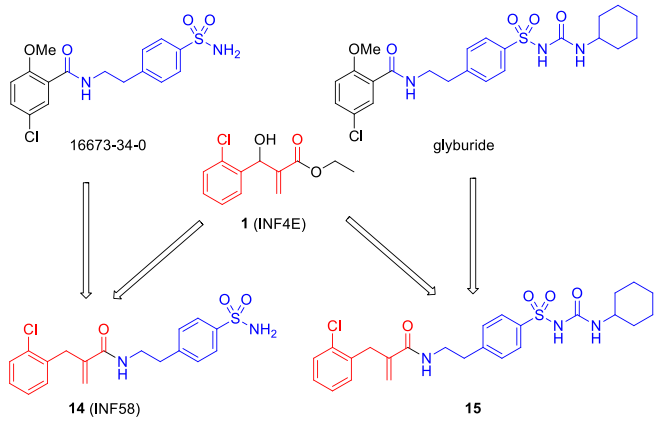

Figure 4. Ligand merging design of compounds **14** (INF58) and **15**.

Results and Discussion

Chemistry

To synthesize acrylamides **4**−**7**, bearing a hydroxyl group in benzylic position, we first followed the route previously described for the synthesis of compound **4**, employing the HBTU/HOBt mediated coupling of 2-((2-chlorophenyl)hydroxy)methyl)acrylic acid (**2**, Figure 1) with *n*-propylamine.[22] However, the use of this route with other primary amines gave rise to a complex mixture of products with no possibility to obtain the desired compounds with a purity >95 % by chromatography. This could be due to the presence of the highly reactive OH group in compound **2**. To overcome this inconvenience we followed a different route (Scheme 1). The hydroxyl group in compound **1** was protected using *tert*-butyldimethylsilyl chloride (TBDMS-Cl) and the obtained intermediate **17** was subsequently hydrolyzed with LiOH in a CH_3CN/H_2O mixture to afford **18** in 70 % yield from **1**. The obtained acid **18** was coupled with the appropriate amine using dicyclohexylcarbodiimide (DCC) and *N*-hydroxysuccinimide (NHS), affording derivatives **19a**−**d**. Derivatives **19a**−**c** were deprotected using tetrabutylammonium fluoride (TBAF) in THF to give the

desired compounds **4**−**6** in good overall yields (41 - 49 %). Compound **19d** was treated with CF_3COOH to remove both the TBDMS- and BOC-protection to afford the desired acrylamide **7**.

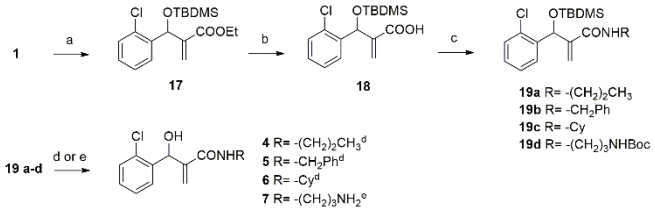

Scheme 1. *Reagents and conditions*: a) TBDMS-Cl (1.5eq), Im (2.5 eq), DMF, RT, 16 h; b) LiOH (10 eq), CH_3CN/H_2O 1/1, 60 °C, 16 h; c) (i): DCC (1 eq), NHS (1 eq), DIPEA (1.5 eq) THF, 0 °C 15 min, RT, 2 h, (ii) amine (2 eq), RT, 16 h; d) TBAF (1.1 eq), THF, RT, 1 h; e) CF_3COOH, DCM, RT, 2 h.

Acrylamides **8**−**14**, lacking the hydroxyl group at the benzylic position, were synthesized using the route depicted in Scheme 2.
Commercially available 2-chlorobenzyl bromide was reacted with ethyl(diethoxyphosphoryl)acetate to afford the phosphonate **20**, which underwent Horner-Wadsworth-Emmons reaction with paraformaldehyde to afford compound **21**. The acrylic ester **21** was hydrolyzed with NaOH to obtain the acid **22**, which was then converted to the activated ester **23** using DCC and NHS. The *N*-hydroxysuccinimidyl ester **23** was purified by flash chromatography and reacted with the selected amines to obtain derivatives **8**−**10**, **12**−**14** in 20 – 32 % overall yields.

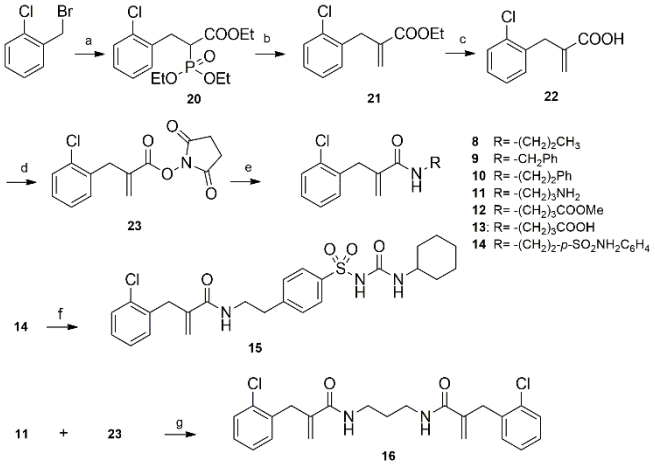

Scheme 2.*Reagents and conditions*: a) ethyl (diethoxyphosphoryl)acetate (1.2 eq), NaH (1.4 eq), DMF, 0 °C, 1 h , RT 18 h; b) paraformaldehyde (6.5 eq), K_2CO_3 (3eq), H_2O, 90 °C, 16 h; c) NaOH, EtOH, RT, 16 h; d) DCC (1eq), NHS (1 eq), THF, 0 °C, 16 h; e) for compounds **8**-**10**, **12**-**14**: H_2N-R (1.5 eq), DCM/DMF 2/1, Et_3N (2 eq), RT, 2-16 h; for compound **11**: (i) H_2N-R (1.5 eq), DCM/DMF 2/1, Et_3N (2 eq), RT, 3 h; (ii) CF_3COOH (10%), DCM, RT, 1 h; f) cyclohexylisocyanate (1.6 eq.), K_2CO_3 (3 eq.), dry acetone, reflux, 16 h; g) DIPEA (1.2 eq.), DMF, RT, 1 h.

To obtain the final compound **11**, a deprotection step performed using 10 % CF_3COOH in CH_2Cl_2 was further required. The sulfonylurea derivative **15** was synthesized by reacting sulfonamide **14** with cyclohexylisocyanate in basic medium. Finally derivative **16**, bearing two electrophilic moieties, was obtained by direct coupling of **11** with stoichiometric amount of **23** and excess diisopropylethylamine (DIPEA) (Scheme 2).

Reactivity as Michael acceptor

The acrylamide functionality has been used in the development of covalent kinase inhibitors.[26] Covalent inhibitors can possess advantages over their reversible counterparts, such as increased biochemical efficiency, longer duration of action, the potential to avoid drug resistance mechanism and the potential for improved efficacy which could reflect in lower therapeutic doses.[23]
However, covalent protein modification has also been implicated in immunotoxicity and idiosyncratic reactions. This kind of toxicity is particularly evidenced if the covalent inhibitor is highly reactive and/or lacks of specificity.[27,28] To rationally design electrophiles for covalent inhibition it is useful to tune both their intrinsic reactivity and non-covalent protein-inhibitor interactions, to optimize selectivity against the desired target(s).

Accordingly, the electrophilic reactivity of the synthesized compounds **4**−**16** and of reference compound **1** was checked using the kinetic cysteamine chemoassay previously described.[22]
Compounds were mixed with an equimolar amount of cysteamine (CAM) in pH 7.4 phosphate-buffered solution at 37 °C using CH_3CN (12.5 %) as the cosolvent. The progress of the reaction was monitored adding 5,5′-dithio-bis(2-nitrobenzoic acid) (DTNB reagent) at different time points over a period of 90 min. None of the tested acrylamides proved reactive under the conditions used. The reference compound **1** showed a k_2 value of 0.824 ± 0.017 M^{-1} s^{-1} with acetonitrile as the cosolvent (k_2 = 0.866 ± 0.006 M^{-1} s^{-1} using DMSO 2.5 % as the cosolvent),[22] while compound **4**, which was previously found to slowly react with CAM using DMSO (k_2 = 0.126 ± 0.005 M^{-1} s^{-1})[22] was unreactive with less polar acetonitrile. These data indicate that the reactivity of this series of electrophilic compounds was efficiently tuned down by employing the acrylamide functionality.
To demonstrate the ability of these acrylamides to behave as Michael acceptors, a model compound (**14**) was reacted with 10 molar equivalents of CAM in pH 7.4 phosphate-buffered solution at 37 °C using CH_3CN as the cosolvent. The decrease in compound **14** concentration was monitored by UHPLC for 7h. Consumption of the electrophile was detected and plotted as the natural log to check for linearity and pseudo-first-order reaction kinetics, $k_{pseudo1st}$.[29] Under these conditions compound **14** was indeed able to slowly react with CAM, with a $k_{pseudo1st}$ of 0.627 ± 0.013 min^{-1} x 10^{-3} (Figure S1).
Finally, in order to evaluate the potential of this class of compounds to trigger idiosyncratic hypersensitivity reactions, all the compounds were checked for their ability to bind human serum albumin. Compounds were added into fresh human serum at 1 mM concentration (CH_3CN < 10% v/v) and incubated for 3 h at 37 °C. Serum aliquots were diluted 200 fold into H_2O/CH_3CN/HCOOH (70/30/0.1% v/v/v), centrifuged and analyzed by ESI-MS as previously reported.[30] None of the acrylamide derivatives was able to covalently react with albumin. On the contrary, compound **1** produced the modification of 65 ± 5% of albumin by generation of three covalent adducts.

Collectively these data show that the reactivity of this class of compounds was decreased to a level which should not promote adverse idiosyncratic reactions mediated by unspecific binding to human serum albumin.

Pharmacology

Anti-pyroptotic activity and cytotoxicity

Synthesized compounds were initially evaluated for their ability to prevent the NLRP3-dependent pyroptosis of phorbol myristate acetate (PMA)-differentiated THP-1 cells. In this model, the NLRP3 inflammasome-dependent events follow a two-stage process. In the first stage (*priming*) NLRP3 expression is induced through a NF-κB-mediated signaling. In the second (*activation*) NLRP3 inflammasome is assembled and activated, following cell exposure to different stimuli. In our experiments, THP-1 cells were primed with LPS and activated with ATP, as previously described.[22] Cell death was quantified by measuring lactate dehydrogenase (LDH) activity in the cell supernatants. First, to perform a preliminary comparative evaluation, cells were exposed (1 h before the ATP pulse) to the synthesized compounds (**4**−**16**; all at 10 μM). The anti-pyroptotic effects were determined and expressed as pyroptosis decrease in comparison with vehicle alone-treated cells (Table 1).

Table 1. Inhibitory effect of compounds **1** (INF4E), **4**-**16** on pyroptotic cell death of THP-1 cells and cytotoxic properties in THP-1 cells.

Compound	Pyroptosis decrease (%) ± SEM[a]	Cytotoxicity TC_{50} ± SEM (μM)[b]	*c*LogP[c]
1 (INF4E)	80.9 ± 5.2	67.0 ± 3.4	2.59
4	31.2 ± 6.8	83.5 ± 2.2	2.09
5	69.8 ± 2.6	44.5 ± 1.2	2.75
6	45.9 ± 5.2	43.4 ± 5.2	3.07
7	35.8 ± 5.3	> 100	0.97[d]
8	7.5 ± 5.6	> 100	3.06
9	28.0 ± 6.6	> 100	3.78
10	49.6 ± 5.7	> 100	4.10
11	15.7 ± 0.7	46.5 ± 5.5	1.94[d]
12	34.7 ± 3.5	> 100	2.77
13	38.5 ± 10.8	> 100	2.31[d]
14 (INF58)	45.8 ± 2.9	> 100	2.27
15	17.3 ± 2.8	> 100	4.40
16	25.2 ± 8.1	> 100	4.75

[a] Determined by measuring LDH release in PMA-differentiated and LPS-primed (5 μg/mL; 4 h) THP-1 cells. Compounds were administered at 10 μM. After 1 h pyroptosis was triggered with ATP (5 mM). LDH activity was measured 1 h after ATP challenge. Data are expressed as percentage of pyroptosis decrease ± SEM vs vehicle aloneof three independent experiments. [b] THP-1 cells were exposed to increasing concentrations (0.1 – 100 μM) of each compound, and cell viability was measured at 72 h by the MTT assay; TC_{50} is the molar conc. of compounds decreasing cell viability by 50%. Data are expressed as the mean ± SEM of three independent experiments. [c] Calculated with ChemBioDraw Ultra 12.0, CambridgeSoft; [d] *c*LogP calculated for the neutral form.

Moreover, as structurally related compounds were demonstrated to exert significant cytotoxicity,[22] the effects of increasing concentrations of the newly synthesized derivatives on the viability of THP-1 cells were evaluated (Table 1).

The ATP-triggered cell death of THP-1 cells (48.0 ± 6.8% pyroptosis *vs* untreated cells) was prevented by both compound **1** (positive control; 80.9 ± 5.2%) and the new acrylamide derivatives; their effects ranged from 7.5 ± 5.6% to 69.8 ± 2.6%. Compounds **4**, **5**, and **7**, bearing a hydroxyl group in X position (structure **I**), exerted higher anti-pyroptotic effects compared to the corresponding analogues **8**, **9** and **11** lacking the hydroxyl group (see **4** *vs* **8**, **5** *vs* **9**, and **7** *vs* **11** in Table 1). Higher intrinsic reactivity, although not measureable with the employed assay, might be responsible for the enhanced anti-pyroptotic effect of the oxygenated series of compounds. In agreement with this hypothesis, the reactivity of α-methyl-*N*-arylacryalmides was recently shown to be increased by introducing a hydroxyl group at the α-carbon atom.[29] Notably, a marked decrease in cell viability was measured when THP-1 cells were cultured in the presence of the α-hydroxyalkyl-substituted acrylamides **4**–**6** (TC_{50} 43.4 ± 5.2 – 83.5 ± 2.2 μM), whereas higher TC_{50} (>100 μM) were generally determined for compounds lacking OH in X position (Table 1). These results indicate that removing OH in α-position decreases cytotoxicity of these acrylamide derivatives. Consequently, further development of OH-substituted compounds was discontinued, and the chemical modulation of the *N*-substituent was carried out using compound **9** (anti-pyroptotic effect = 28.0 ± 6.6%; TC_{50} >100 μM) as the preferred scaffold. In addition, compound **8**, lacking a significant anti-pyroptotic activity, was also considered as a model to gather a more complete insight into the activity of this class of compounds.

To evaluate whether the higher activity of **9** compared to **8** could be attributed to the increased lipophilicity (*c*LogP = 3.78 and 3.06, respectively), *N*-phenylethyl derivative **10** (*c*LogP = 4.10) was synthesized. Compared with compound **9**, this derivative exerted larger anti-pyroptotic effects (49.6 ± 5.7%), thus confirming the hypothesis that the relative anti-pyroptotic activity of these related compounds could depend on their lipophilicity. In addition, when the *N*-propyl chain in **8** was

substituted with an amino group at the terminal position, a less lipophilic, still poorly active, and more cytotoxic compound (**11**) was obtained (*c*LogP = 1.94; anti-pyroptotic effect = 15.7 ± 0.7%; TC_{50} = 46.5 ± 5.5 μM). The activity was slightly increased when a methoxycarbonyl (**12**) or a carboxy group (**13**) were introduced in the same position (Table 1). Of note, compared with compound **8**, derivatives **11**−**13** are more hydrophilic (*c*LogP = 1.94 – 2.77), thus indicating that factors other than lipophilicity alone are likely responsible for the pharmaco-toxicological activity of these derivatives. Consistently, compound **16**, formally obtained by dimerization of **8**, exerted only modest anti-pyroptotic effects (25.2 ± 8.1%), in spite of a high degree of lipophilicity (*c*LogP = 4.75). Finally, to further insight into the SAR of the acrylamide moiety, the effects exerted by compounds **14** and **15** were studied. Interestingly, 16673-34-0-derived compound **14** exerted effects (45.8 ± 2.9% pyroptosis inhibition) comparable to those of **10** despite the decreased lipophilicity (*c*LogP = 2.27), while highly lipophilic glyburide-derived compound **15** (*c*LogP = 4.40) exerted only modest anti-pyroptotic effects in our model (17.3 ± 2.8% pyroptosis inhibition). To better characterize the anti-pyroptotic activity of these acrylamides, the concentration-response curve of representative derivatives (compounds **8**−**10**, **12**, and **14**) was studied (Figure 5).

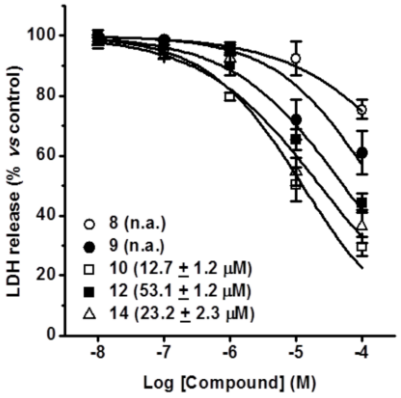

Figure 5. Concentration-response curves of anti-pyroptotic effect for compounds **8**, **9**, **10**, **12**, and **14**; IC_{50} values ± SEM are reported in brackets; n.a.= not-applicable. Data are the mean ± SEM of three independent experiments.

The ATP-triggered pyroptosis of THP-1 cells was prevented by these compounds in a concentration-dependent manner: the IC_{50} ranged from 12.7 to 53.1 μM.
Collectively, these data demonstrate that weak electrophiles, obtained by chemical modulation of structure **I** (X=H), can be efficiently used to design and develop non-toxic NLRP3 inhibitors acting as anti-pyroptotic agents.

Inhibition of IL-1β release from macrophages

We next verified the ability of most interesting compounds to inhibit NLRP3-dependent IL-1β secretion in macrophages. Murine immortalized bone marrow-derived macrophages (BMDMs), primary BMDMs, and primary inflammatory peritoneal macrophages were primed with LPS and then treated with extracellular ATP in order to activate NLRP3 (Figure 6). Compounds **5**, **10**, **12**, **14**, and **16** were added to the macrophages either simultaneously to LPS treatment, or 15 min prior to ATP pulse. All tested compounds significantly inhibited IL-1β secretion when added simultaneously with LPS regardless of the type of macrophages (Figure 6). Most compounds were also effective when added 15 min only before ATP treatment, suggesting that these compounds block NLRP3 activation in ATP-driven second step and not LPS-dependent priming. Consistently, none of the compounds affect TLR4-dependent NLRP3-independent TNF-α release demonstrating that they do not target activation of inflammatory genes transcription triggered by LPS.

Inhibition of IL-1β release from CAPS mutant macrophages

Gain-of-function mutations in the *NLRP3* gene cause hereditary autoinflammations referred to as CAPS that correspond to a disease spectrum of three clinically defined disorders: familial cold autoinflammatory syndrome (FCAS), Muckle-Wells syndrome (MWS), and neonatal-onset multisystem inflammatory disease (NOMID). In order to evaluate the potential of these compounds in CAPS treatment, we tested their ability to dampen the activity of CAPS-associated NLRP3 mutants. We reconstituted mouse immortalized NLRP3 KO BMDMs with murine NLRP3 R258W and A350V (corresponding to the human R260W and A352V mutations respectively, both associated

with MWS) and NLRP3 L351P (corresponding to the human L353P mutation associated with FCAS).[31-33] As previously described,[34,35] LPS priming is sufficient to trigger IL-1β secretion from macrophages expressing NLRP3 R258W, A350V, and L351P. Compounds **10**, **12**, and **14**, selected for this kind of experiments, inhibited ATP-dependent IL-1β secretion in LPS-primed macrophages expressing WT NLRP3 (Figure 7). Compound **10** inhibited LPS-induced IL-1β secretion by macrophages expressing NLRP3 R258W, A350V, and L351P. Compound **14** inhibited LPS-induced IL-1β secretion by macrophages expressing NLRP3 R258W and L351P, while compound **12** effect was restricted to macrophages expressing R258W.

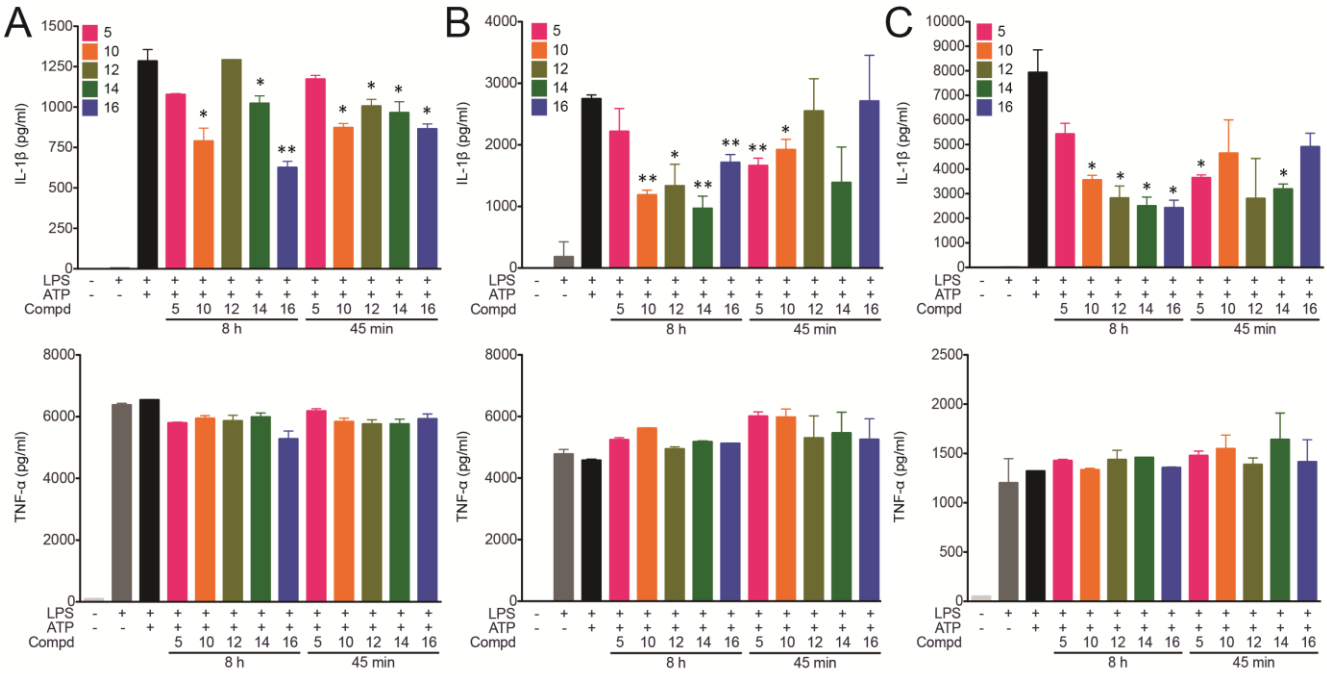

Figure 6. Effect of compounds **5**, **10**, **12**, **14**, and **16** on IL-1β and TNF-α release in murine immortalized macrophages (**A**), bone marrow derived macrophages (**B**), and primary peritoneal macrophages (**C**). Macrophages were treated with LPS (50 ng/mL, 8 h) and ATP (2mM, 30 min). Compounds (20 µM) were added simultaneously with LPS (8 h) or 15 min before ATP treatment (45 min total). Secretion of IL-1β and TNF-α in culture supernatant were measured by ELISA. * $P < 0.05$; ** $P < 0.01$ vs LPS and ATP treated cells; t-test. Values are the mean ± SD. Results are representative of two independent experiments performed both in duplicate.

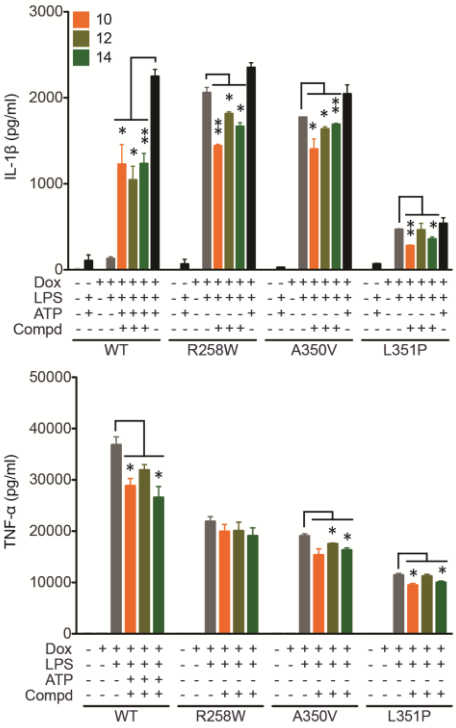

Figure 7. Effect of compounds **10**, **12** and **14** on IL-1β and TNF-α released by BMDMs expressing NLRP3 WT, R258W, A350V or L351P mutants. Immortalized murine NLRP3 KO BMDMs reconstituted with WT or mutant NLRP3 were treated with doxycycline (0.1 µg/mL, 24 h), LPS (50 ng/mL, 8 h) and ATP (2 mM, 30 min).

Compounds (20 µM) were added simultaneously with LPS (8 h). Secretion of IL-1β and TNF-α in culture supernatant were measured by ELISA. * P < 0.05; ** P < 0.01 vs LPS treated cells in mutant BMDMs; * P < 0.05; ** P < 0.01 vs LPS and ATP in WT BMDMs; t-test. Values are the mean ± SD. Results are representative of two independent experiments performed both in duplicate.

Inhibition of NLRP3 ATPase activity

The ability of compounds **5**, **10**, **12**, and **14** to inhibit the NLRP3 ATPase activity was tested on purified human recombinant enzyme. Human recombinant NLRP3 was incubated at 37 °C in the presence of different concentrations (50 µM, 100 µM) of tested compounds for 15 min. ATP was then added and mixture incubated at 37 °C for further 40 min. The amount of ATP converted to ADP was determined by luminescence using the ADP-Glo assay. The obtained results, expressed as percentage of residual enzyme activity with respect to vehicle treated enzyme, are reported in Figure 8A. All the compounds inhibited NLRP3 ATPase activity when tested at 100 µM, while only derivatives **5** and **14** inhibited the enzyme at 50 µM. We next verified the ability of compound **14**, able to prevent pyroptotic cell death and to inhibit IL-1β release from different macrophage lines and devoid of significant toxicity, to concentration-dependently inhibit ATPase activity of NLRP3 protein (Figure 8B). The enzymatic activity was indeed decreased in a concentration-dependent manner with a calculated IC_{50} of 74 µM (C.L. 95 = 63-86 µM) demonstrating that NLRP3 is a direct target of compound **14** (INF58).

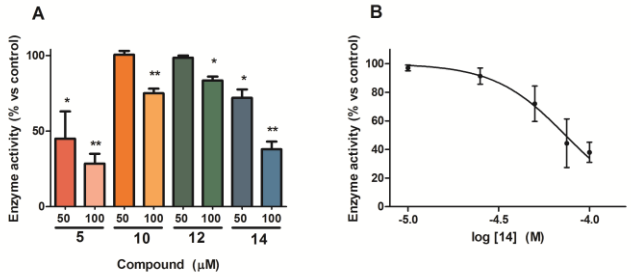

Figure 8. A) Inhibition of NLRP3 ATPase activity of selected compounds **5**, **10**, **12**, **14**; Values are the mean ± SEM of three independent experiments.* P < 0.05; ** P < 0.01 vs vehicle treated enzyme; t-test. B) concentration-response curve for derivative **14** (INF58).

Computational studies

As discussed above, compound **14**, and other analogues from this class of acrylamide derivatives, proved able to inhibit NLRP3 ATPase activity. We then applied a computational approach to predict the putative binding mode of **14**, and other synthesized compounds, in the ATP binding pocket in the NACHT domain of NLRP3. As explained in Methods and depicted in Figure 9 (in orange), a preliminary docking analysis involved the natural ligand ATP with a view to further assessing the reliability of the modeled binding pocket. Satisfactorily, the computed complex is in line with the data reported in the literature [36] since the phosphate groups are seen to stabilize ion-pair with Lys232 and Arg237 plus H-bonds with Thr233 and His522. Arg237 also contacts the ATP adenine base whose 6-amino group elicits a reinforced H-bond with Lys238. Lastly, the ATP sugar moiety is engaged in H-bonds with Tyr381 and to a minor extent with Trp416.

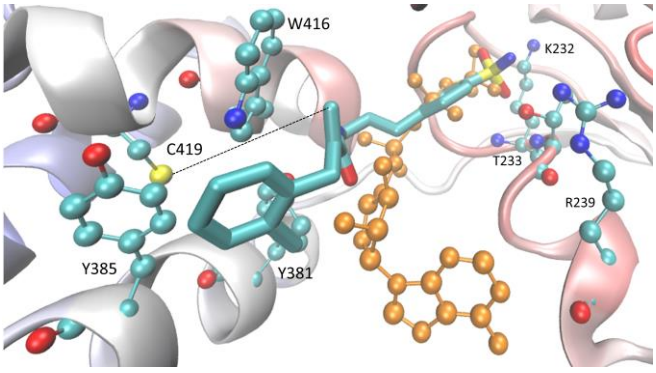

Figure 9. Comparison of the putative poses as computed for ATP (in orange) and **14** (INF58, in light blue). The dashed black line defines the path between the supposedly reactive Cys419 residue and the β carbon atom of the acrylamide group.

As shown in Figure 9 (in light blue), compound **14** is accommodated in the regions of the binding site which harbor the ribose ring and the phosphate groups of ATP where it can elicit a set of key interactions which can be schematized as follows.
The 2-chlorophenyl moiety is engaged in extended π-π stacking interactions with surrounding aromatic residues such as Tyr381, Tyr385 and Trp416. This last residue also contacts the reactive vinyl group of the acrylamide moiety and might have a key role in approaching the reactive ligand moiety to Cys419 (see below). The amide oxygen atom is involved in a clear H-bond with Tyr381, while the phenyl sulfonamide moiety mimics the ATP phosphate groups stabilizing a rich set of charge transfer interactions and reinforced H-bonds involving Lys232, Thr233, Arg237 and His522. Such an extended network of contacts should maintain the inhibitor in a pose stably conducive to the formation of covalent adduct with the protein. In detail the reactive acrylamide is surrounded by three rather close cysteine residues (i.e. Cys409, Cys415 and Cys419). Among them Cys419 seems to be the most reactive one for two main reasons. Firstly, it is the closest residue since its distance with the acrylamide is equal to 8.3 Å (the corresponding distances for Cys409 and Cys415 are equal to 14.9 Å and 11.1 Å, respectively) and between Cys419 and the acrylamide there are no residues which can obstruct the approaching, while the hypothetic path for Cys409 and Cys415 is hindered by other residues as exemplified by Pro412. Secondly, Cys419 is surrounded by residues, such as Tyr385, which should enhance its reactivity by stabilizing its thiolate form with a mechanism already seen for albumin and glutathione transferase enzymes.[37]
The other simulated derivatives show comparable poses all characterized by the capacity to insert the 2-chlorophenyl ring in the above described subpocket lined by several aromatic residues which have the dual role of stabilizing the complex and of constraining the acrylamide moiety in a pose conducive to the Michael addition. Notably, the obtained docking results and in particular the observed interactions stabilized by the varying moieties linked to the acrylamide nitrogen atom can offer additional explanations for the measured ATPase activity. Indeed, compounds **5**, **10** and **12** reveal putative complexes very similar to that observed for **14** in which the reinforced H-bonds with Lys232 and Arg237 are replaced by extended charge transfer interactions with the distal phenyl ring in **5** and **10**, and by H-bonds with the ester group in compound **12**.

Conclusions

With the aim to obtain covalent NLRP3 inhibitors, we designed and synthesized a series of acrylamide derivatives endowed with low intrinsic electrophilicity, which reflected in avoided unspecific idiosyncratic and cytotoxic effects. Most of the synthesized compounds prevented ATP-triggered, NLRP3-dependent pyroptotic cell death of PMA differentiated THP-1 cells, showing no significant cytotoxicity. The obtained results allowed the selection of compounds **10**, **12**, and **14**, able to prevent pyroptosis in a concentration-dependent manner, and endowed with a promising pharmaco-toxicological profile. Derivatives **10**, **12**, and **14** were able to inhibit IL-1β release from different macrophages lines, with no effect on TLR-4 dependent TNF-α production. Compounds **10**, **12**, and **14** were also effective in inhibiting IL-1β release from macrophages bearing CAPS-associated NLRP3 mutants. Compound **14** (INF58) inhibited NLRP3 ATPase activity with an IC_{50} of 74 μM, resulting in a good hit compound to design new and improved direct NLRP3 inhibitors. *In silico* prediction of the binding mode of **14** in the ATPase catalytic pocket indicates that a putative interaction with Cys419 residue might account for this activity. Binding studies to identify the binding site(s) of **14** (INF58) to human recombinant NLRP3 are in progress, results will be reported in due course.

Experimental Section

Chemistry

All the reactions were monitored by TLC on Merck 60 F_{254} (0.25 mm) plates, which were visualized by UV inspection and/or by spraying $KMnO_4$ (0.5 g in 100 ml 0.1 N NaOH). Flash chromatography (FC) purifications were performed using silica gel Fluka with 60 mesh particles. ^{1}H and ^{13}C-NMR spectra were registered on Bruker Avance 300 spectrometer, at 300 and 75 MHz respectively. Coupling constants (*J*) are given in Hertz (Hz) and chemical shifts (δ) are given in ppm, calibrated to tetramethylsilane (TMS) as internal standard. Following abbreviations are used to describe molteplicities: s= singlet, d= doublet, t= triplet, q= quadruplet, m= multiplet and br= broad signal. Low-resolution mass spectra were recorded on a Finnigan-MAT TSQ700 in chemical ionization mode (CI) using isobutane. Melting points were measured with a capillary apparatus (Büchi 540). Purity of compounds was checked by UHPLC (PerkinElmer) Flexar 15, equipped with UV-Vis diode array detector using an Acquity UHPLC CSH Phenyl-Hexyl 1.7 µm 2.1×50 mm column (Waters) and H_2O/CH_3CN and H_2O/CH_3OH solvent systems. Detection was performed at λ= 200, 215 and 254 nm. The analytical data confirmed that the purity of the products was ≥95%.

Ethyl 2-(((*tert*-butyldimethylsilyl)oxy)(2-chlorophenyl)methyl)acrylate (17): to a stirred solution of **1**[22] (2.41 g, 10 mmol) in DMF (3mL) imidazole (1.70 g, 25 mmol) was added. After complete dissolution, *tert*-butyldimetylsilylchloride (2.26 g, 15 mmol) was added portionwise and the solution was stirred overnight at room temperature. Water (20 mL) was added and the mixture was extracted with EtOAc (3 × 30 mL), washed with brine, dried (Na_2SO_4), filtered and concentrated under reduced pressure. Purification by silica gel chromatography eluting with 9:1 PE/EtOAc gave **17** as a colourless oil (2.91 g, 82%): R_f= 0.87 (PE/EtOAc 9:1); ^{1}H NMR (300 MHz, $CDCI_3$) δ= 7.44-7.11 (m, 4H), 6.28 (s, 1H), 6.05 (s, 1H), 5.82 (s, 1H), 4.09 (q, *J*= 7.1 Hz, 2H), 1.17 (t, *J*= 7.1 Hz, 3H), 0.85 (s, 9H), 0.09 (s, 3H) -0.12 ppm (s, 3H); ^{13}C NMR (75 MHz, $CDCl_3$) δ= 168.5, 146.2, 142.9, 135.6, 132.2, 132.1, 131.5, 129.6, 127.9, 71.9, 63.5, 28.6, 21.0, 17.0, -2.0, -2.1 ppm; MS (CI, isobutane) *m/z* (%): 357 (32), 355 (100) $[M+H]^+$.

2-(((*Tert*-butyldimethylsilyl)oxy)(2-chlorophenyl)methyl)acrylic acid (18): compound **17** (2.91 g, 8.20 mmol) was dissolved in 1:1 CH_3CN/H_2O (20 mL) and LiOH (1.96 g, 82.0 mmol) was added. The reaction was stirred at 60 °C overnight. The solvent was evaporated under reduced pressure. The residue was diluted with 1N HCl (10 mL), and extracted with EtOAc (4 × 25 mL). The combined organic phases were washed with brine, dried (Na_2SO_4), filtered and concentrated under reduced pressure. Purification by silica gel chromatography eluting with DCM/MeOH from 97:3 to 9:1 gave **18** as a colourless oil (2.28 g, 85%): R_f= 0.68 (DCM/MeOH 9:1);^{1}H NMR (300 MHz, $CDCI_3$) δ= 10.04 (br, 1H), 7.50 (d, *J*= 7.8 Hz,1H), 7.32-7.16 (m, 3H), 6.42 (s, 1H), 6.03 (s, 1H), 5.85 (s, 1H), 0.87 (s, 9H), 0.10 (s, 3H), -0.09 ppm (s, 3H); ^{13}C NMR (75 MHz, $CDCl_3$) δ= 171.2, 142.9, 140.2, 133.3, 130.0, 129.7, 129.4, 128.6, 127.4, 69.5, 26.4, 28.8, -4.2, -4.3 ppm. MS (CI, isobutane) *m/z* (%): 329 (37), 327 (100) $[M+H]^+$.

General procedure for the synthesis of compounds 19 (a-d): the carboxylic acid **18** (0.456 mg, 1.39 mmol) was dissolved in THF (10 mL), then DIPEA (0.364 mL, 2.10 mmol) and DCC (0.288 g, 1.39 mmol) were added. The mixture was stirred for 15 min at 0 °C and for further 2h at room temperature. Appropriate amine (2 eq.) was then added and the reaction stirred overnight at room temperature. The mixture was filtered and the liquid phase extracted with EtOAc (4 × 30 mL). The organic phases were washed with saturated NH_4Cl solution (20 mL), dried (Na_2SO_4), filtered and evaporated. The products were purified by silica gel chromatography, eluting with PE/EtOAc 9:1.

2-(((*Tert*-butyldimethylsilyl)oxy)(2-chlorophenyl)methyl)-*N*-propylacrylamide (19a): the reaction was run using propylamine (0.228 mL, 2.78 mmol) obtaining **19a** as a colourless oil (0.317 g, 62%): R_f= 0.74 (PE/EtOAc 8:2);^{1}H NMR (300 MHz, $CDCI_3$) δ= 7.55 (d, *J*= 7.8 Hz,1H),7.29-7.19 (m, 3H), 6.68 (br, 1H), 5.95 (s, 1H), 5.92 (s, 1H), 5.53 (s, 1H), 3.24-3.21 (m, 2H), 1.55-1.48 (m, 2H), 0.90 (s, 9H), 0.87 (t, *J*= 7.1 Hz, 3H), 0.12 (s, 3H), -0.02 ppm (s, 3H); ^{13}C NMR (75 MHz, $CDCl_3$) δ= 166.6, 144.4, 138.9, 132.2, 129.6, 128.8, 128.3, 126.7, 121.6, 72.1, 41.1, 25.7, 22.8, 18.1, 11.5, 0.0, -5.0 ppm; MS (CI, isobutane) *m/z* (%): 370 (32), 368 (100) $[M+H]^+$.

2-(((*Tert*-butyldimethylsilyl)oxy)(2-chlorophenyl)methyl)-N-cyclohexylacrylamide (19b): the reaction was run using cyclohexylamine (0.190 mL, 2.78 mmol) obtaining **19b** as a yellowish oil (0.420 g, 74%): R_f= 0.72 (PE/EtOAc 9:1);^{1}H NMR (300 MHz, $CDCI_3$) δ= 7.67 (d, *J*= 7.6 Hz, 1H), 7.35-7.23 (m, 3H), 6.26 (br, 1H), 5.85 (s, 1H), 5.76 (s, 1H), 5.33 (s, 1H), 1.93-1.83 (m, 2H), 1.75-1.58 (m, 3H), 1.41-1.32 (m, 2H), 1.22-1.13 (m, 4H), 0.96 (s, 9H), 0.24 (s, 3H), -0.21 ppm (s, 3H); ^{13}C NMR (75 MHz, $CDCl_3$) δ= 168.6, 144.8, 141.9, 131.2, 129.4, 128.5, 128.0, 127.1, 122.6, 74.1, 51.6, 43.3, 31.0, 25.9, 25.7, 24.0, -0.5, -4.0 ppm; MS (CI, isobutane) *m/z* (%): 410 (32), 408 (100) $[M+H]^+$.

***N*-Benzyl-2-(((*tert*-butyldimethylsilyl)oxy)(2-chlorophenyl)methyl)acrylamide (19c)**: the reaction was run using benzylamine (0.304 mL, 2.78 mmol) obtaining **19c** as a yellowish oil (0.468 g, 81%): R_f= 0.70 (PE/EtOAc 9:1);^{1}H NMR (300 MHz, $CDCI_3$) δ= 7.39-7.15 (m, 9H), 6.23 (br, 1H), 5.79 (s,1H), 5.31 (s, 1H), 5.18 (s, 1H), 3.87 (s, 2H), 0.94 (s, 9H), 0.22 (s, 3H), -0.33 ppm (s, 3H); ^{13}C NMR (75 MHz, $CDCl_3$) δ= 168.2, 143.1, 138.9, 136.3, 134.6, 131.5, 130.0, 129.1, 128.4, 128.0, 127.8, 127.3, 121.1, 73.8, 44.1, 32.0, 25.7, -1.5, -3.9 ppm; MS (CI, isobutane) *m/z* (%): 418 (32), 416 (100) $[M+H]^+$.

***Tert*-butyl (3-(2-(((tert-butyldimethylsilyl)oxy)(2-chlorophenyl)methyl)acrylamido)propyl) carbamate (19d)**: the reaction was run using *N*-BOC-1,3-propanediamine (0.484 g, 2.78 mmol) obtaining **19d** as a pale white oil (0.403 g, 60%): R_f= 0.61 (PE/EtOAc 9:1);^{1}H NMR (300 MHz, $CDCI_3$) δ= 7.35-7.13 (m, 4H), 7.03 (br, 1H), 5.79 (s,1H), 5.63 (s, 1H), 5.25 (br, 1H), 5.10 (s, 1H), 3.33 (t, *J*= 7.1 Hz, 2H), 3.08 (t, *J*= 8.1 Hz, 2H), 1.61-1.57 (m, 2H), 1.42 (s, 9H), 0.96 (s, 9H), 0.18 (s, 3H), -0.32 ppm (s, 3H); ^{13}C NMR (75 MHz, $CDCl_3$) δ= 168.7, 156.6, 142.4, 136.3, 134.0, 131.1, 129.5, 128.0, 126.7, 119.7, 79.2, 74.2, 37.0, 36.3, 31.1, 30.0, 28.5, 25.7, -1.5, -3.8 ppm; MS (CI, isobutane) *m/z* (%): 485 (32), 483 (100) $[M+H]^+$.

General procedure for synthesis of compounds 4- 7: to a solution of compound **19a-d** (0.70 mmol) in dry THF (5 mL), tetrabutylammonium fluoride (1.0 M in THF, 0.77 mL, 0.77 mmol) was added at 0 °C. The mixture was stirred for 1h at room temperature and then diluted with water (15 mL) and extracted with DCM (3x 20mL). The organic phases were washed with brine, water (20 mL), dried (Na_2SO_4), filtered and evaporated. The products were purified by silica gel chromatography, eluting with 95:5 PE/ EtOAc.

2-((2-Chlorophenyl)(hydroxy)methyl)-*N*-propylacrylamide (4): compound **4** was obtained as a white solid (0.169 g, 95%) starting from **19a**: characterization data were in agreement with previously reported data.[20]

***N*-Benzyl-2-((2-chlorophenyl)(hydroxy)methyl)acrylamide (5)**: compound **5** was obtained as a white solid (0.169 g, 80%) starting from **19b**: R_f= 0.52 (PE/EtOAc 85:15); mp: 94.3-95.6 °C; ^{1}H NMR (300 MHz, $CDCI_3$) δ= 7.63 (d, *J*= 7.6 Hz, 1H), 7.33-7.14 (m, 8H), 6.78 (br, 1H), 5.85 (d, *J*= 4.9 Hz, 1H), 5.78 (s, 1H), 5.30 (s, 1H), 3.57 (d, , *J*= 5.1 Hz ,1H), 3.16 ppm (s, 2H); ^{13}C NMR (75 MHz, $CDCl_3$) δ= 168.4, 143.2, 138.5, 136.6, 134.8, 131.7, 129.9, 129.1, 128.6, 128.1, 127.7, 127.4, 120.1, 66.7, 44.0 ppm; MS (CI, isobutane) *m/z* (%): 304 (32), 302 (100) $[M+H]^+$.

2-((2-Chlorophenyl)(hydroxy)methyl)-*N*-cyclohexylacrylamide (6): compound **6** was obtained as a white solid (0.179 g, 87%) starting from **19c**: R_f= 0.41 (PE/EtOAc 9:1); mp: 119.4-120.8 °C; ^{1}H NMR (300 MHz, $CDCI_3$) δ= 7.69 (d, *J*= 7.6 Hz, 1H), 7.34-.7.23 (m, 3H), 6.27 (br, 1H), 5.84 (s, 1H), 5.76 (s, 1H), 5.30 (s, 1H), 4.28 (br, 1H), 1.94-1.87(m, 2H), 1.75-1.60 (m, 3H), 1.41-1.32 (m, 2H), 1.22-1.13 ppm (m, 4H); ^{13}C NMR (75 MHz, $CDCl_3$) δ= 168.6, 144.6, 142.1, 131.2, 129.3, 128.3, 127.7, 127.0, 122.3, 66.7, 51.5, 43.3, 25.7, 24.2 ppm; MS (CI, isobutane) *m/z* (%): 296 (32), 294 (100) $[M+H]^+$.

3-(2-((2-Chlorophenyl)(hydroxy)methyl)acrylamido)propan-1-aminium 2,2,2-trifluoroacetate (7): **19d** was dissolved in CH_2Cl_2 (5mL) and trifluoroacetic acid (0.500 mL, 6.49 mmol) was added dropwise. The mixture was stirred at room temperature for 2h and then concentrated to dryness. The white solid was washed several times with CH_2Cl_2 and diethylether and **7** was obtained as a white amorphous solid (140.6 mg, 99%); ^{1}H NMR (300 MHz, D_2O) δ= 7.47-7.29 (m, 4H), 5.83 (s,1 H), 5.76 (s, 1H), 5.26 (s, 1H), 3.17-3.11 (m, 2H), 2.71 (t, *J*= 7.1 Hz, 2H), 1.69-1.55 ppm (m, 2H); ^{13}C NMR (75 MHz, D_2O): δ= 172.5, 142.2, 136.1, 134.1, 131.3, 129.9, 128.7, 127.5, 121.2, 118.5, 114.8, 68.9, 40.5, 34.4, 26.9 ppm.

Ethyl 3-(2-chlorophenyl)-2-(diethoxyphosphoryl)propanoate (20): to a stirred solution of ethyl (diethoxyphosphoryl)acetate (7.86 g, 35.1 mmol) in DMF (30 mL) at 0 °C, NaH (60 % in mineral oil) (1.64 g, 41.0 mmol) was added and the mixture stirred for 1h at 0 °C. To the obtained mixture 2-chlorophenylmethyl bromide (6.00 g, 29.3 mmol) was added at 0 °C, and the reaction was stirred for 18h at room temperature. The reaction mixture was quenched with water and extracted with EtOAc (50 mL × 3). The combined organic layers were washed with water (50 mL), brine (50 mL), dried (Na_2SO_4), and evaporated. Purification by silica gel chromatography eluting with PE /EtOAc (from 7:3 to 1:1) gave **20** as a colorless oil (7.25 g, 71%): R_f= 0.29 (PE/EtOAc 7:3); ^{1}H NMR (300 MHz, $CDCI_3$) δ= 7.36-7.09 (m, 4H), 4.26-4.06 (m, 6H), 3.52-3.27 (m, 3H), 1.39-1.33 (m, 6H), 1.15 ppm (t, *J*= 7.0 Hz, 3H).[38]

Ethyl 2-(2-chlorobenzyl)acrylate (21): to a stirred mixture of **20** (7.25 g, 20.8 mmol) and paraformaldehyde (4.13 g, 137mmol) in water (60 mL) a solution of potassium carbonate (8.62 g. 62.4 mmol) in water (60 mL) was added at room temperature. The mixture was stirred overnight at 90 °C. After cooling to room temperature, the mixture was extracted with EtOAc (3 × 50 mL), and the organic layer was washed with brine (50 mL), dried (Na_2SO_4), filtered and evaporated. Purification by silica gel chromatography eluting with PE/EtOAc 7:3 gave **21** as a colorless oil (3.06 g, 66%): R_f= 0.45 (PE/EtOAc 95:5);^{1}H NMR (300 MHz, $CDCI_3$) δ= 7.50-6.99 (m, 4H), 6.27 (d, *J*= 0.9 Hz,1 H), 5.33 (d, *J*= 1.2 Hz, 1H), 4.22 (q, *J*= 7.1 Hz, 2H), 3.76 (s, 2H), 1.29 ppm (t, *J*= 7.1 Hz, 3H); ^{13}C NMR (75 MHz, $CDCl_3$) δ= 166.8, 138.4, 136.4, 134.5, 131.2, 129.6, 127.9, 126.8, 126.3, 60.4, 35.4, 14.2 ppm; MS (CI, isobutane) *m/z* (%): 227 (32), 225 (100) $[M+H]^+$.

2-(2-Chlorobenzyl)acrylic acid (22): to a stirred solution of **21** (3.06 g, 19.6 mmol) in EtOH (5 mL) 2.5 M NaOH was added (1.3 mL) and the reaction was stirred at room temperature overnight. The mixture was diluted with 10% $NaHCO_3$ (15 mL) and extracted with EtOAc (15 mL). The aqueous phase was acidified with 1M HCl and extracted with EtOAc (3 × 20 mL). The organic phases were dried (Na_2SO_4), filtered and evaporated. Compound **22** was obtained as a white solid (2.54 g, 95%): mp: 90.5-91.5 °C; ^{1}H NMR (300 MHz, $CDCI_3$) δ= 11.84 (br, 1H),7.37-7.14 (m, 4H), 6.41 (s,1H), 5.44 (s, 1H), 3.74 ppm (s, 2H); ^{13}C NMR (75 MHz, $CDCl_3$) δ= ^{13}C NMR (75 MHz, $CDCI_3$) δ 172.4, 137.9, 136.5, 134.9, 131.6, 130.1, 129.4, 128.5, 127.3, 35.4 ppm. MS (CI, isobutane) *m/z* (%): 199 (32), 197 (100) $[M+H]^+$.

2,5-Dioxopyrrolidin-1-yl, 2-(2-chlorobenzyl)acrylate (23): to a stirred solution of **22** (2.39 g, 12.1 mmol) in dry THF (25 mL) *N*,*N'*-dicyclohexylcarbodiimide (2.50 g, 12.1 mmol) was added at 0 °C. After 10 min, *N*-hydroxysuccinimide (1.39 g, 12.1 mmol) was added at the same temperature and the reaction was stirred at room temperature overnight. The

mixture was filtered and the liquid phase extracted with EtOAc (3 × 30 mL). The organic layer was washed with saturated NH_4Cl solution (15 mL), dried (Na_2SO_4), filtered and evaporated. Purification by silica gel chromatography eluting with CH_2Cl_2/ EtOAc 99:1 gave **23** as a white solid (3.00 g, 84%): R_f= 0.37 (CH_2Cl_2/EtOAc 99:1); mp: 131.7-133.2 °C; ^{1}H NMR (300 MHz, $CDCl_3$) δ= 7.38-7.18 (m, 4H), 6.55 (s,1H), 5.62 (s, 1H), 3.80 (s, 2H), 2.82 ppm (s, 4H); ^{13}C NMR (75 MHz, $CDCl_3$):δ= 169.7, 135.3, 134.9, 134.2, 131.6, 130.3,130.1, 129.4, 128.5, 127.3, 35.7, 26.0 ppm; MS (CI, isobutane) *m/z* (%): 296 (32), 294 (100) [*M*+H]$^+$.

General procedure for the synthesis of compounds 8-14: to a stirred solution of **23** (0.29 g, 1.00 mmol) in 2:1 DCM/DMF (6 mL) an excess of the appropriate amine (2.00 mmol) was added at room temperature followed by triethylamine (3.00 mmol). The reaction mixture was stirred at room temperature for 2h-24h. The mixture was diluted with water (30 mL), acidified with 1N HCl (20 mL), then extracted with EtOAc (4 × 30 mL). The organic phase was washed with brine, dried (Na_2SO_4), filtered and evaporated to obtain the crude product.

2-(2-Chlorobenzyl)-*N*-propylacrylamide (8): propylamine (118.2 mg, 2.00 mmol) was used as the reacting amine and the reaction mixture was stirred for 6h. Purification by silica gel chromatography eluting with DCM to 99:1 DCM/EtOAc gave **8** as a pale yellow oil (183.5 mg, 77%): R_f= 0.63 (DCM/EtOAc 9:1); ^{1}H NMR (300 MHz, $CDCl_3$) δ= 7.37-7.17 (m, 4H) 5.92 (br, 1H), 5.71 (s,1 H), 5.11 (s, 1H), 3.78 (s, 2H), 3.24 (t, *J*= 7.1 Hz, 2H), 1.51 (m, 2H), 0.87 ppm (t, *J*= 7.2 Hz, 2H); ^{13}C NMR (75 MHz, $CDCl_3$): δ= 166.9, 140.4, 137.3, 134.3, 128.6, 128.5, 127.2, 126.9, 124.3, 40.8, 37.1, 23.2, 11.2 ppm; MS (CI, isobutane) *m/z* (%): 240 (32), 238 (100) [*M*+H]$^+$.

***N*-Benzyl-2-(2-chlorobenzyl)acrylamide (9)**: benzylamine (214.3 mg, 2.00 mmol) was used as the reacting amine and the reaction mixture was stirred for 8h. Purification by silica gel chromatography eluting with DCM to 98:2 DCM/EtOAc gave **9** as a white solid (157.2 mg, 56%): R_f= 0.81 (DCM/EtOAc 9:1); mp: 87.1-88.0 °C; ^{1}H NMR (300 MHz, $CDCl_3$) δ= 7.38-7.21 (m, 9H), 6.23 (br, 1H), 5.76 (s,1H), 5.18 (s, 1H), 4.50 (s, 2H), 3.84 (s, 2H); ^{13}C NMR (75 MHz, $CDCl_3$): δ= 168.4, 143.2, 138.5, 136.4, 134.8, 131.7, 130.0, 129.1, 128.5, 128.1, 127.9, 127.4, 120.1, 44.1, 36.3 ppm; MS (CI, isobutane) *m/z* (%): 288 (32), 286 (100) [*M*+H]$^+$.

2-(2-Chlorobenzyl)-*N*-phenethylacrylamide (10): phenethylamine (242.4mg, 2.00 mmol) was used as the reacting amine and the reaction mixture was stirred for 12h. Purification by silica gel chromatography eluting with 9:1 DCM/EtOAc gave **10** as a white solid (158.9 mg, 53%): R_f= 0.71 (DCM/EtOAc 9:1; mp: 66.5-68.0 °C; ^{1}H NMR (300 MHz, CDCl*3*) δ= 7.34-7.09 (m, 9H), 5.90 (br, 1H), 5.61 (s, 1H), 5.07 (s,1H), 3.73 (s, 2H), 3.52 ppm (t, *J*= 7.1 Hz, 2H), 2.78 ppm (t, *J*= 7.1 Hz, 2H); ^{13}C NMR (75 MHz, $CDCl_3$) δ= 168.8, 140.2, 139.3, 137.4, 134.2, 130.6, 129.3,128.7, 128.5, 127.7, 127.2, 125.9, 124.2, 40.8, 37.1, 35.2 ppm; MS (CI, isobutane) *m/z* (%): 302 (32), 300 (100) [*M*+H]$^+$.

***N*-(3-Aminopropyl)-2-(2-chlorobenzyl)acrylamide trifluoroacetate (11)**: *tert*-butyl (3-aminopropyl)carbamate (348.5 mg, 2.00 mmol) was used as the reacting amine and the reaction mixture was stirred for 3h. Purification by silica gel chromatography eluting with 1:1 PE/EtOAc gave the Boc-protected **11** as a white solid (264.7 mg, 75%). This intermediate (148.7 mg, 0.422 mmol) was dissolved in DCM (5mL) and trifluoroacetic acid (0.500 mL, 6.49 mmol) was added. The mixture was stirred at room temperature for 1h and concentrated to dryness. The white solid was washed several times with CH_2Cl_2 and diethylether, and **11** was obtained as a white crystalline solid (134.5 mg, 87%), trifluoroacete: R_f= 0.23 (DCM/MeOH 1:1); mp: 118.1-119.0 °C; ^{1}H NMR (300 MHz, D_2O) δ= 7.30 (d, *J*= 7.5 Hz, 1H), 7.13-7.10 (m, 3H), 5.54 (s,1H), 5.24 (s, 1H), 3.61 (s, 2H), 3.11 (t, *J*= 6.5 Hz, 2H), 2.54 (t, *J*= 6.6Hz, 2H), 1.67-1.55 (m, 2H), 1.66-1.50 (m, 4H), 1.23-0.87 ppm (m, 6H); ^{13}C NMR (75 MHz, D_2O): δ= 172.5, 142.2, 136.1, 134.1, 131.3, 129.9, 128.7, 127.5, 121.2, 118.5, 114.8, 40.5, 36.6, 34.4, 26.9 ppm.

Methyl 4-(2-(2-chlorobenzyl)acrylamido)butanoate (12): methyl 4-aminobutanoate hydrochloride (307.2 mg, 2.00 mmol) was used as the reacting amine and the reaction was stirred for 16h. Purification by silica gel chromatography, eluting with 7:3 PE/EtOAC to 1:1 PE/EtOAc gave **12** as a white solid (162.7 mg, 55%): R_f= 0.64 (PE/EtOAc 1:1); mp: 69.5-71.0 °C; ^{1}H NMR (300 MHz, $CDCl_3$) δ= 7.38-7.18 (m, 4H), 6.16 (br, 1H), 5.72 (s,1H), 5.12 (s, 1H), 3.77 (s, 2H), 3.67 (s, 3H), 3.34 (t, *J*= 7.1 Hz, 2H), 2.32 (t, *J*= 7.1 Hz, 2H), 1.88-1.79 ppm (m, 2H); ^{13}C NMR (75 MHz, $CDCl_3$): δ=174.4, 168.6, 143.2, 136.5, 134.7, 131.6, 130.0, 128.5, 127.4, 119.9, 52.2, 39.6, 36.2, 31.9, 24.8 ppm; MS (CI, isobutane) *m/z* (%): 298 (32), 296 (100) [*M*+H]$^+$.

4-(2-(2-Chlorobenzyl)acrylamido)butanoic acid (13): 4-aminobutanoic acid (206.2 mg, 2.00 mmol) was used as the reacting amine and the reaction mixture was stirred in 1:1 DCM/DMF for 24h. Purification by silica gel chromatography eluting with 99:1 DCM/MeOH gave **13** as a white solid (128.9 mg, 66%): R_f= 0.80 (DCM/MeOH 1:1); mp: 68.5-70.3 °C; ^{1}H NMR (300 MHz, $CDCl_3$): δ= 10.60 (br, 1H), 7.33-7.17 (m, 4H), 6.56 (br, 1H), 5.72 (s, 1H), 5.09 (s, 1H), 3.73 (s, 2H), 3.32 (t, *J*= 7.1 Hz, 2H), 2.31 (t, *J*= 7.1 Hz, 2H), 1.85-1.76 ppm (m, 2H); ^{13}C NMR (75 MHz, $CDCl_3$): δ= 178.2, 168.3, 142.7, 136.4, 134.7, 131.6, 130.0, 128.6, 127.4, 120.5, 39.6, 36.1, 31.9, 24.7 ppm.

2-(2-Chlorobenzyl)-*N*-(4-sulfamoylphenethyl)acrylamide (14): 4-(2-aminoethyl)-benzenesulphonamide (400.5 mg, 2.00 mmol) was used as the reacting amine and the reaction mixture was stirred in DMF for 12h. Purification by silica gel chromatography eluting with DCM to 7:3 DCM/EtOAc gave **14** as a white solid (223.5 mg, 59%): R_f= 0.43 (DCM/EtOAc 1:1); mp: 150.3-151.1 °C; ^{1}H NMR (300 MHz, CD_3OD) δ= 7.79 (d, *J*= 8.0 Hz, 2H), 7.44-7.28 (m, 4H), 7.22 (d, *J*= 9.1 Hz, 2H), 5.66 (s,1 H), 5.11 (s, 1H), 3.72 (s, 2H), 3.47 (t, *J*= 7.1 Hz, 2H), 2.88 ppm (t, *J*= 7.1 Hz, 2H); ^{13}C NMR (75 MHz, CD_3OD): δ= 168.5, 142.9, 141.6, 140.4, 135.0, 132.9, 129.7, 128.0, 127.9, 126.8, 125.6, 124.7, 117.9, 39.2, 34.2, 33.5 ppm; MS (CI, isobutane) *m/z* (%): 381 (32), 379 (100) $[M+H]^+$.

2-(2-Chlorobenzyl)-*N*-(4-(*N*-(cyclohexylcarbamoyl)sulfamoyl)phenethyl)acrylamide (15): compound **14** (98.7 mg, 0.261 mmol) was dissolved in dry acetone in a N_2 atmosphere and K_2CO_3 (108.0 mg, 0.732 mmol) was added portionwise. After 1.5h of reflux stirring, cyclohexyl isocianate (52.0 mg, 0.417 mmol) dissolved in dry acetone (20 mL) was added dropwise to the reaction mixture. The reaction was refluxed overnight. After cooling, the mixture was added with water (15 mL), and acidified to pH 1 with 1N HCl. The obtained white precipitate was collected and recrystallized from. methanol to afford **15** as a white solid (51.0 mg, 39%): R_f= 0.43 (DCM/EtOAc 1:1); mp: 166.7-168.5 °C; ^{1}H NMR (300 MHz, DMSO-$_{d6}$) δ= 10.34 (br, 1H), 8.25 (s, 1H), 7.79 (d, *J*= 8.0 Hz, 2H) 7.44-7.28 (m, 6H), 6.39 (d, *J*= 7.7 Hz, 1H), 5.69 (s,1 H), 5.03 (s, 1H), 3.65 (s, 2H), 3.38 (t, *J*= 6.9 Hz, 2H), 3.33-3.30 (m, 1H), 2.84 (t, *J*= 6.8 Hz, 2H), 1.66-1.50 (m, 4H), 1.23-0.87 ppm (m, 6H); ^{13}C NMR (75 MHz, DMSO-$_{d6}$): δ= 168.1, 150.5, 146.1, 139.0, 137.4, 134.2, 131.9, 130.1, 129.9, 129.1, 128.1, 128.0, 127.7, 120.0, 48.9, 40.7, 36.1, 35.5, 33.2, 22.8, 25.1 ppm; MS (CI, isobutane) *m/z* (%): 505 (32), 503 (100) $[M+H]^+$.

***N,N*'-(Propane-1,3-diyl)bis(2-(2-chlorobenzyl)acrylamide) (16)**: compound **11** (91.0 mg, 0.249 mmol) was dissolved in DMF (5mL) and DIPEA (51 µL, 0.299 mmol) was added dropwise. The mixture was stirred for 10 min at room temperature, then **23** (61.0 mg, 0.208 mmol) was added and the reaction mixture stirred for 1h at room temperature. The reaction was diluted with 1N HCl (10mL) and extracted with CH_2Cl_2 (3 × 25mL). The organic phases were dried (Na_2SO_4), filtered and evaporated under reduced pressure. Purification by silica gel chromatography eluting with 98:2 CH_2Cl_2/MeOH gave **16** as a white solid (75.0 mg, 84%): R_f= 0.30 (DCM/MeOH 98:2); mp: 138.8-140.3 °C; ^{1}H NMR (300 MHz, $CDCl_3$) δ= 7.61-6.94 (m, 8H), 6.61 (br, 2H), 5.79 (s, 2H), 5.17 (s, 2H), 3.69 (s, 4H), 3.19 (t, *J*= 6.2 Hz, 4H), 1.67-1.46 ppm (m, 2H); ^{13}C NMR (75 MHz, $CDCl_3$): δ= 168.7, 142.7, 136.1, 134.4, 131.2, 129.6, 128.1, 126.9, 119.7, 35.9, 35.5, 29.5 ppm; MS (CI, isobutane) *m/z* (%):432(64), 430 (100) $[M+H]^+$.

Kinetic cysteamine chemoassay: The thiol assay was performed in 96-well plates using 100 mM phosphate buffer (pH 7.4) with 500 µM EDTA as the solvent system. DTNB reagent was prepared with 0.014 mmol DTNB (Sigma-Aldrich, Saint Luis, MO, USA) and 0.5 mmol sodium hydrogencarbonate dissolved in 25 mL 100 mM phosphate buffer (pH 7.2). All measurements were done in a Multilabel Plate Reader (Victor X4, Perkin Elmer, Waltham, MA, USA) at 37 °C. To perform the assay, CH_3CN solutions of compounds (10 mM) and water solution of cysteamine (CAM) (Sigma-Aldrich) (10 mM) were diluted in the phosphate buffer to give a concentration of 0.5 mM. An equal amount of both solutions were combined, mixed and the kinetic measurements started immediately. At various time points (over a time of 90 minutes) 150 µL of DTNB reagent were added and after one minute absorption was measured at λ= 405 nm. The concentration of the remaining reduced CAM was determined via a CAM calibration curve of thiol content *vs.* absorbance (CAM concentration ranging from 0.03 to 0.35 mM). Rate constants of reaction between CAM and the electrophilic compounds were determined as reported.[22]

Reaction of compound 14 with cysteamine: The electrophilic reactivity of compound **14** was quantified in terms of pseudo-first-order reaction rate constant, $k_{pseudo\ 1st}$, employing cysteamine (CAM) as a nucleophile. The reaction vessel contained 500 µM electrophile and 5 mM CAM in 100 mM potassium phosphate buffer (pH 7.4) with 25% acetonitrile as cosolvent. The stirred reaction mixture was maintained at 37 ± 0.5 °C for 7h. At different time intervals 500 µL of this solution were analyzed by RP-UHPLC using a Flexar UHPLC (Perkin Elmer) equipped with a Flexar Solvent Manager 3-CH-Degasser, a Flexar-FX UHPLC autosampler, a Flexar-FX PDA UHPLC Detector, a Flexar-LC Column Oven, and a Flexar-FX-15 UHPLC Pump. The analytical column was an Acquity CSH^{TM} (2.1 x 100 mm, 1.7 µm particle size) (Waters) column. The samples were analyzed using an isocratic method employing a mobile phase consisting of methanol/buffer (70/30) (flow rate 0.2 mL/min). The column effluent was monitored at λ= 204 nm referenced against a λ= 360 nm. Quantification was done using calibration curves of compound **14** chromatographed under the same conditions. The linearity of the calibration curves was determined in a concentration range of 100 - 1000 µM ($r^2 > 0.98$). Data analysis was performed using Chromera Manager (Perkin Elmer). All experiments were run in triplicate. The pseudo-first-order rate constant was determined by plotting the natural log of the concentration of **14** as a function of time. The negative slope of the straight line is the pseudo-first-order rate constant. The $k_{pseudo1st}$ was then calculated according to the reported method.[29]

Albumin modification test: The analytic platform was composed of a Surveyor LC system, which was connected to a TSQ Quantum Ultra mass spectrometer through a Finnigan IonMax electrospray ionization (ESI) source assembled with a low flow stainless steel emitter (Thermo Fisher Scientific, Rodano, MI, Italy). Each compound was dissolved in acetonitrile and tested separately. Compounds were spiked into fresh human serum down to a concentration equal to 1 mM. The spiked volume was less than 10% of serum volume to avoid protein precipitation. The temperature was kept at 37 °C throughout the incubation time (3h). Before the analysis, serum aliquots were diluted 200 fold into $H_2O/CH_3CN/HCOOH$ (70/30/0.1; v/v/v). Samples were then centrifuged for 10 minutes at 18000g and the supernatant was placed in clear glass vials and kept at 4 °C in the autosampler compartment. The analyses were performed by an automated loop injection method and sampling was programmed as a 50 µL-partial-loop injection performed by the HPLC

system. Once loaded into the sample loop, samples were pushed at a flow rate of 25 µL/min through a peek tube directly connected to the ESI source. The mobile phase isocratic flow was delivered by the pump at the final composition $H_2O/CH_3CN/HCOOH$ (70/30/0.1; v/v/v). The analyzer was operating in conditions similar to the reported ones.[27] Briefly, MS spectra were acquired for 5 minutes by a TSQ Quantum Ultra mass spectrometer in positive ion mode using the following settings: ESI voltage 3.5 KV, capillary temperature 300 °C, sheath gas 35%, Q3 scan range 1410-1500 m/z, Q3 power 0.4 amu, scan time 1 second, Q2 gas pressure 1.5 torr, skimmer offset 10 V, microscan set to 3. Full instrument control and extraction of albumin ESI mass spectra were provided by Xcalibur software (version 2.0.7, Thermo Fisher Scientific, Rodano, MI, Italy). Mass spectra deconvolution was provided by MagTran software (version 1.02).[39] Covalent adducts were detected depending upon the expected molecular weights (i.e. adduct molecular weight=albumin molecular weight+compound molecular weight). The amount of modified albumin was then calculated from the relative abundance of unmodified protein and adducts.

Biological studies

***In vitro* models of pyroptosis**: Pyroptosis was studied as previously described.[22] The day before each experiment, cells were plated in 48-well culture plates (75×10^3 cells/well) and were differentiated into monocyte-macrophages-like cells by treatment with PMA (50 nM; 24h; Sigma-Aldrich). PMA-differentiated THP-1 cells were washed twice with phosphate-buffered saline (PBS) and primed with LPS (5 µg/mL; 4h; Sigma-Aldrich) in serum-free medium. Cell death was triggered with ATP (5 mM; 1h; Sigma-Aldrich). Cell death was quantified by using the CytoTox 96 Non-Radioactive Cytotoxicity Assay (Promega Corporation, Madison, MI, USA), based on a colorimetric measurement of LDH activity in the collected supernatants. Cell death was expressed according to the manufacturer's instruction.

Cytotoxicity assay: THP-1 cells were plated in 96-wells culture plates (5×10^3 cells/well) and exposed to increasing concentrations (0.1-100 µM) of each compound. The cultures were maintained at 37 °C, 95 % air/5 % CO_2 in a fully humidified incubator. Cell viability was measured at 72h by the MTT assay.

Mice: C57Bl/6J mice were housed at the PBES Facility (ENS Lyon). Experiments were performed in accordance with european and institutional guidelines. Inflammatory peritoneal macrophages were elicited by the intraperitoneal injection of 4 % thioglycolate broth for 4 days.

Constructs: Mouse NLRP3 cDNA was amplified by PCR from cDNAs of C57Bl/6Jmouse macrophages. cDNAs coding for R258W, A350V and L351P NLRP3 mutants were obtained from mouse NLRP3 cDNA by PCR (QuickChange II Site-directed Mutagenesis kit, Agilent Technologies) using the following oligos:
mNLRP3_R258W_F:ctatttgttctttatccactgctgggaggtgagcctcaggac;
mNLRP3_R258W_R:gtcctgaggctcacctcccagcagtggataaagaacaaatag;
mNLRP3_A350V_F:cataacgacgaggccggtagtcttggagaaactgcagcatc;
mNLRP3_A350V_R:gatgctgcagtttctccaagactaccggcctcgtcgttatg;
mNLRP3_L351P_F:cgacgaggccggtagccccggagaaactgcagcatctc;
mNLRP3_L351P_R:gagatgctgcagtttctccggggctaccggcctcgtcg; WT, R258W, A350V and L351P NLRP3 cDNAs were cloned in GFP encoding pInducer21 under doxycycline-dependent promotor for lentiviral vector production.

Cell culture: Immortalized WT and NLRP3 KO bone marrow-derived macrophages BMDMs were a kind gift from Dr E. Alnemri (Jefferson University). Immortalized NLRP3 KO BMDMs were reconstituted with WT, R258W, A350V or L351P NLRP3 by lentiviral transduction followed by flow cytometry sorting of GFP-positive cells. Inflammatory peritoneal macrophages and immortalized BMDMs were cultured at $0.5 – 1 \times 10^6$ cells/ml in Dulbecco's modified Eagle's Medium (DMEM) supplemented with 1× penicillin/streptomycin (PS) and 10 % Fetal Bovine Serum (FBS) (Gibco). Primary BMDMs were cultured at $0.5\text{-}1 \times 10^6$ cells/ml in DMEM supplemented with 10 % FBS, 10 % M-CSF conditioned media, 1 % Hepes and 1 % Na-pyruvate, 1 % glutamine. Cells were treated with doxycycline (Sigma), LPS from Escherichia coli 0111:B4 (Sigma) and ATP (Sigma).

ELISA test: mIL-1β and mTNF-α assays were performed using the DuoSet ELISA kits (R&D Systems).

Measurement of NLRP3-ATPase Activity: Human recombinant NLRP3 (0.105 µg; BPS Bioscience, San Diego, USA) was incubated with the assessed compounds in the reaction buffer (20 mM Tris-HCl, pH 7.8, 133 mM NaCl, 20 mM $MgCl_2$, 3 mM KCl, 0.56 mM EDTA, DMSO 0.5 %) for 15 min at 37 °C. ATP (250 µM, Ultra Pure ATP) was added and the reaction mixtures were further incubated for 40 min at 37 °C. The hydrolysis of ATP by NLRP3 was determined by a luminescent ADP detection performed with ADP-Glo™ Kinase Assay (Promega, Madison, USA) according to the manufacturer's protocol.

Computational methods

Docking simulations involved the NACHT domain of the human NLPR3 protein (residues 220-536, Entry Id: Q96P20, Entry Name: NLRP3_HUMAN) the homology model of which was generated by using the resolved structure of NLRC4 (PDB Id: 4KXF). Briefly, the homology modelling was performed by Modeller 9.10 using the default parameters;[36] among the 20 generated models, the best structure was selected according to the computed scores (i.e. DOPE and GA341) as well as to the percentage of residues falling in the allowed regions of the Ramachandran (91.2 %) and chi plots (95.8 %). The selected model was carefully checked to avoid unphysical occurrences such as cis peptide bonds, wrong configurations, improper bond lengths, non-planar aromatic rings or colliding side-chains. To remain compatible with physiologic pH, Asp, Glu, Lys and Arg residues were considered in their ionized forms, while His and Cys residues were

maintained neutral by default. The so completed model underwent to a minimization procedure keeping fixed the backbone atoms to preserve the predicted folding and the so obtained final structure was utilized in the following docking simulations which involved ATP, taken as a reference ligand, plus the here reported inhibitors. The ATP structure was retrieved from the resolved structure (PDB Id=4AFF) which shows the best resolution among those co-crystallized with ATP and its conformation was optimized by PM7 semi-empirical method as implemented in MOPAC2012. In contrast, the conformational profile of the here reported inhibitors was explored by MonteCarlo simulations which generated 1000 minimized geometries by randomly rotating the rotatable bonds. The so obtained lowest energy structure underwent the following docking simulations which were performed by using PLANTS and arranged in two steps.[40] The first step involved the docking of ATP whose search was focused on a 12 Å radius sphere around the highly conserved Lys232 residue the key role of which was confirmed by previous studies. The so computed complex was then minimized by keeping fixed all atoms outside a 12 Å radius sphere around the bound ATP and the so optimized NLPR3 structure was used in the docking analyses of the reported inhibitors by focusing the search on a 12 Å radius sphere around the bound ATP. In all docking simulations, 20 poses were generated and scored by using the ChemPLP score function with speed equal to 1. The computed best complexes for the proposed inhibitors were optimized with the same protocol already described for the ATP complex.

Acknowledgements

This work was supported by Università degli Studi di Torino, Ric. Loc. 2014 and 2015 and in part by the French National Research Agency (ANR-13-JSV3-0002-01 to BP) and the European Research Council (ERC-2013-CoG_616986 to BP). Authors wish to thank Dr. E. Alnemri (Jefferson University) for the kind share of immortalized WT and NLRP3 KO murine bone marrow-derived macrophages, Dr. E. Lupino (Università degli Studi di Torino) for kind assistance in the NLRP3 ATPase assay, and Dr. M. L. Lolli (Università degli Studi di Torino) for access to UHPLC instrument.

Keywords: acrylamide derivatives • CAPS • covalent drugs • NLRP3 inflammasome • pyroptosis.

References:

[1] G. Y. Chen, G. Nunez, *Nat. Rev. Immunology* **2010**, *10*, 826-837.
[2] O. Takeuchi, S. Akira, *Cell* **2010**, *140*, 805-820.
[3] P. Pelegrin, A. Suprenant, *EMBO J.* **2006**, *25*, 5071-5082.
[4] S. Locovei, E. Scemes, F. Qui, D. Spray, G. Dahl, *FEBS Lett.* **2007**, *581*, 483-488.
[5] V. Compan, A. Baroja-Mazo, G. Lopez-Castejon, A. Gomez, C. M. Martinez, D. Angosto, M. T. Montero, A. S. Herranz, E. Bazan, D. Reimers, V. Mulero, P. Pelegrin, *Immunity* **2012**, *37*, 487-500.
[6] V. Compan, F. Martın-Sanchez, A. Baroja-Mazo, G. Lopez-Castejon, A. I. Gomez, A. Verkhratsky, D. Brough, P. Pelegrın, *J. Immunol.* **2015**, *194*, 1261-1273.
[7] P. Duewell, H. Kono, K. J. Rayner, C. M. Sirois, G. Vladimer, F. G. Bauernfeind, G. S. Abela, L. Franchi, G. Nunez, M. Schnurr, T. Espevik, E. Lien, K. Fitzgerald, A. Rock, K. J. Moore, S. D. Wright, V. Hornung, E. Latz, *Nature* **2010**, *464*, 1357−1361.
[8] F. Martinon, V. Petrilli, A. Mayor, A. Tardivel, J. Tschopp, *Nature* **2006**, *440*, 237−241.
[9] A. Halle, V. Hornung, G. C. Petzold, C. R. Stewart, B. G. Monks, T. Reinheckel, K. A. Fitzgerald, E. Latz, K. J. Moore, D. T. Golenbock, *Nat. Immunol.* **2008**, *9*, 857−865.
[10] M. Lamkanfi, V. M. Dixit, *Cell* **2014**, *157*, 1013-1022.
[11] F. S. Sutterwala, S. Haasken, S. L. Cassel, *Ann. N.Y. Acad. Sci*. **2014**, *1319*, 82-95.
[12] H. Guo, J. B. Callaway, J. P-Y. Tang, *Nat. Med.* **2015**, *21*, 677-687.
[13] L. Agostini, K. Burns, M. F. McDermott, P. N. Hawkins, J. Tschopp, *Immunity* **2004**, *20*, 319-325.
[14] R. Goldbach-Mansky, N. J. Dailey, S. W. Canna, A. Gelabert, J. Jones, B. I. Rubin, H. J. Kim, C. Brewer, C. Zalewski, E. Wiggs, S. Hill, M. L. Turner, B. I. Karp, I. Aksentijevich, F. Pucino, S. R. Penzak, M. H. Haverkamp. L. Stein, B. Adams, T. L. Moore, R. C. Fuhlbrigge, B. Shaham, J. N. Jarvis, K. O'Neil, R. K. Vehe, L. O. Beitz, G. Gardner, W. P. Hannan, R. W. Warren, W. Horn, J. L. Cole, S. M. Paul, P. N. Hawkins, T. H. Pham, C. Snyder, R. A. Wesley, S. C. Hoffmann, S. M. Holland, J. A. Butman, D. L. Kastner, *N. Engl. J. Med.* **2006**, *355*, 581-592.
[15] M. Gattorno, S. Tassi, S. Carta, L. Delfino, F. Ferlito, M. A. Pelagatti, A. D'Osualdo, A. Buoncompagni, M. G. Alpigiani, M. Alessio, A. Martini, A. Rubartelli, *Arthritis Rheum*. **2007**, *56*, 3138-3148.
[16] A. Baroja-Mazo, F. Martín-Sánchez, A. I Gomez, C. M. Martínez, J. Amores-Iniesta, V. Compan, M. Barberà-Cremades, J. Yagüe, E. Ruiz-Ortiz, J. Antón, S. Buján, I. Couillin, D. Brough, J. I. Arostegui, P. Pelegrín, *Nat. Immunol.* **2014**, *15*, 738-750.
[17] H. M. Lee, J. J. Kim, H. J. Kim, M. Shong, B. J. Ku, E. K. Jo, *Diabetes* **2013**, *62*, 194−204.
[18] M. T. Heneka, M. P. Kummer, A. Stutz, A. Delekate, S. Schwartz, A. Vieira-Saecker, A. Griep, D. Axt, A. Remus, T. C. Tzeng, E. Gelpi, A. Halle, M. Korte, E. Latz, D. T. Golenbock, *Nature* **2012**, *493*, 674−678.
[19] A. G. Baldwin, D. Brough, S. Freeman, *J. Med. Chem.* DOI:10.1021/acs.jmedchem.5b01091.
[20] J. A. MacDonald, C. P. Wijekoon, K. C. Liao, D. A. Muruve, *IUBMB Life* **2013**, *65*, 851-862.
[21] J. A. Duncan, D. T. Bergstralh, Y. Wang, S. B. Willingham, Z. Ye, A.G. Zimmermann, J. P. Ting, *Procl. Natl. Acad. Sci. U.S.A*. **2007**, *104*, 8041-8046.
[22] M. Cocco, D. Garella, A. Di Stilo, E. Borretto, L. Stevanato, M. Giorgis, E. Marini, R. Fantozzi, G. Miglio, M. Bertinaria, *J. Med. Chem*. **2014**, *57*, 10366-10382.
[23] R. A. Bauer, *Drug Discovery Today* **2015**, *20,* 1061-1073.
[24] C. Marchetti, J. Chojnacki, S. Toldo, E. Mezzaroma, N. Tranchida, S. W. Rose, M. Federici, B. W. Van Tassell, S. Zhang, A. Abbate, *J. Cardiovasc. Pharmacol.* **2014**, *63*, 316−322.
[25] M. Lamkanfi, J. L. Mueller, A. C. Vitari, S. Misaghi, A. Fedorova, A. K. Deshayes, W. P. Lee, H. M. Hoffman, V. M. Dixit, *J. Cell Biol.* **2009**, *187*, 61-70.
[26] M. C. Noe, A. M. Gilbert in *Annu. Rep. Med. Chem. Vol. 47* (Ed. M. C. Desai), Academic Press, San Diego, **2012** pp. 413-439.
[27] J. Uetrecht, *Chem. Res. Toxicol.* **2009**, *22*, 24−34.

[28] X. Zhang, F. Liu, X. Chen, X. Zhu, J. Uetrecht, *Drug Metab. Pharmacokinet.* **2011**, *26*, 47−59.
[29] M. E. Flanagan, J. A. Abramite, D. P. Anderson, A. Aulabaugh, U. P. Dahal, A. M. Gilbert, C. Li, J. Montgomery, S. R. Oppenheimer, T. Ryder, B. P. Schuff, D. P. Uccello, G. S. Walker, Y. Wu, M. F. Brown, J. M. Chen, M. M. Hayward, M. C. Noe, R. S. Obach, L. Philippe, V. Shanmugasundaram, M. J. Shapiro, J. Starr, J. Stroh, Y. Che, *J. Med. Chem.* **2014**, *57*, 10072−10079.
[30] L. Regazzoni, L. Del Vecchio, A. Altomare, K. J. Yeum, D. Cusi, F. Locatelli, M. Carini, G. Aldini, *Free Radical Res.* **2013**, *47*, 172-180.
[31] H. M. Hoffman, J. L. Mueller, D. H. Broide, A. A. Wanderer, R. D. Kolodner, *Nat. Genet.* **2001**, *29*, 301-305.
[32] H. M. Hoffman, J. L. Muller, M. Tresierras, D. H. Broide, A. A. Wanderer, R. D. Kolodner, *Hum. Genet.* **2003**, *112*, 209-216.
[33] C. Dodé, N. Le Du, L. Cuisset, F. Letourneur, J-M. Berthelot, G. Vaudour, A. Meyrier, R. A Watts, D. G. I. Scott, A. Nicholls, B. Granel, C. Frances, F. Garcier, P. Edery, S. Boulinguez, J-P. Domergues, M. Delpech, G. Grateau, *Am. J. Hum. Genet.* **2002**, *70*, 1498-1506.
[34] S. D. Brydges, J. L. Muller, M. D. McGeough, C. A. Pena, A. Misaghi, C. Gandhi, C. D. Putnam, D. L. Boyle, G. S. Firestein, A. A. Horner, P. Soroosh, W. T. Watford, J. J. O'Shea, D. L. Kastner, H. M. Hoffman, *Immunity*, **2009**, *30*, 875-887.
[35] G. Meng, F. Zhang, I. Fuss, A. Kitani, W. Strober, *Immunity* **2009**, *30*, 860-874.
[36] M. A. Marti-Renom, A. Stuart, A. Fiser, R. Sánchez, F. Melo, A. Sali, *Annu. Rev. Biophys. Biomol. Struct.* **2000**, *29*, 291-325.
[37] G. Aldini, G. Vistoli, L. Regazzoni, L. Gamberoni, R. M. Facino, S. Yamaguchi, K. Uchida, M. Carini, *Chem. Res. Toxicol.* **2008**, *21,* 824-835.
[38] Y. Hashizume, M. Hirota, H. Koike, Y. Matsumoto, S. Mihara, H. Nakamura, PCT WO **2006**/134485.
[39] Z. Zhang, A. G. Marshall, *J. Am. Soc. Mass Spectrom.* **1998**, *9*, 225-233.
[40] O. Korb, T. Stützle, T. E. Exner, *J. Chem. Inf. Model.* **2009**, *49*, 84-96.